References and Notes

1. D. J. Begun, H. A. Lindfors, M. E. Thompson, A. K. Holloway, *Genetics* **172**, 1675–1681 (2006).
2. M. T. Levine, C. D. Jones, A. D. Kern, H. A. Lindfors, D. J. Begun, *Proc. Natl. Acad. Sci. U.S.A.* **103**, 9935–9939 (2006).
3. D. J. Begun, H. A. Lindfors, A. D. Kern, C. D. Jones, *Genetics* **176**, 1131–1137 (2007).
4. Q. Zhou et al., *Genome Res.* **18**, 1446–1455 (2008).
5. D. G. Knowles, A. McLysaght, *Genome Res.* **19**, 1752–1759 (2009).
6. W. Xiao et al., *PLOS ONE* **4**, e4603 (2009).
7. J. Cai, R. Zhao, H. Jiang, W. Wang, *Genetics* **179**, 487–496 (2008).
8. A. R. Carvunis et al., *Nature* **487**, 370–374 (2012).
9. T. J. A. J. Heinen, F. Staubach, D. Häming, D. Tautz, *Curr. Biol.* **19**, 1527–1531 (2009).
10. S. Chen, Y. E. Zhang, M. Long, *Science* **330**, 1682–1685 (2010).
11. J. A. Reinhardt et al., *PLOS Genet.* **9**, e1003860 (2013).
12. T. F. C. Mackay et al., *Nature* **482**, 173–178 (2012).
13. See supplementary materials on *Science* Online.
14. N. Sheth et al., *Nucleic Acids Res.* **34**, 3955–3967 (2006).
15. V. N. Uversky, *Protein Sci.* **11**, 739–756 (2002).
16. D. Hebenstreit et al., *Mol. Syst. Biol.* **7**, 497 (2011).
17. D. Schwartz, *Genetics* **67**, 411–425 (1971).
18. R. M. Graze et al., *Mol. Biol. Evol.* **29**, 1521–1532 (2012).
19. J. M. Smith, J. Haigh, *Genet. Res.* **23**, 23–35 (1974).
20. N. L. Kaplan, R. R. Hudson, C. H. Langley, *Genetics* **123**, 887–899 (1989).
21. J. Hermisson, P. S. Pennings, *Genetics* **169**, 2335–2352 (2005).
22. D. J. Begun et al., *PLOS Biol.* **5**, e310 (2007).
23. C. H. Langley et al., *Genetics* **192**, 533–598 (2012).

Crude Oil Impairs Cardiac Excitation-Contraction Coupling in Fish

Fabien Brette,[1] Ben Machado,[1] Caroline Cros,[1] John P. Incardona,[2] Nathaniel L. Scholz,[2] Barbara A. Block[1]*

Crude oil is known to disrupt cardiac function in fish embryos. Large oil spills, such as the Deepwater Horizon (DWH) disaster that occurred in 2010 in the Gulf of Mexico, could severely affect fish at impacted spawning sites. The physiological mechanisms underlying such potential cardiotoxic effects remain unclear. Here, we show that crude oil samples collected from the DWH spill prolonged the action potential of isolated cardiomyocytes from juvenile bluefin and yellowfin tunas, through the blocking of the delayed rectifier potassium current (I_{Kr}). Crude oil exposure also decreased calcium current (I_{Ca}) and calcium cycling, which disrupted excitation-contraction coupling in cardiomyocytes. Our findings demonstrate a cardiotoxic mechanism by which crude oil affects the regulation of cellular excitability, with implications for life-threatening arrhythmias in vertebrates.

Crude oil is a complex chemical mixture containing hydrocarbons (aliphatic and aromatic) and other dissolved-phase organic compounds. Toxicity research on crude oil constituents has focused mainly on polycyclic aromatic hydrocarbons (PAHs) (*1*, *2*), pervasive environmental contaminants that are also found in coal tar, creosote, air pollution, and land-based runoff. In the aftermath of oil spills, PAHs can persist for many years in marine habitats and thereby create pathways for lingering biological exposure and associated adverse effects.

PAH toxicity is structure-dependent, and the carcinogenic, mutagenic, and teratogenic properties of many individual PAHs are known (*3*, *4*). Developing fish are particularly vulnerable to dissolved PAHs in the range of ~100 parts per billion (ppb or μg/liter) down to ≤10 μg/liter. Consequently, PAH toxicity to fish early life stages is an important contributor to both acute and long-term impacts of environmental disasters (*2*, *5*).

Numerous studies on crude oils and PAHs, particularly in the aftermath of the Exxon Valdez spill, have described embryonic heart failure, bradycardia, arrhythmias, reduction of contractility, and a syndrome of cardiogenic fluid accumulation (edema) in exposed fish embryos (*6*, *7*). These severe effects are lethal to embryos and larval fishes (*8*–*10*) and could be due to atrioventricular conduction block (*11*).

Despite recent progress using zebrafish and other experimental models to study PAH cardiotoxicity (*12*), the mechanisms that underpin the physiological effects on cardiac function and changes in cardiac morphology during development are not known. The Deepwater Horizon (DWH) oil spill released >4 million barrels of crude oil during the peak spawning months for Atlantic bluefin tuna (*Thunnus thynnus*) in 2010. This large and long-lived species reaches a mass of 650 kg over a life span of 35 years or more (*13*), and the Gulf of Mexico population of bluefin tuna is severely depleted (*14*). Electronic-tagging data confirm that bluefin tuna spawn in the vicinity of the DWH spill, which indicates that bluefin tuna embryos, larvae, juveniles, and adults were likely exposed to crude oil–derived PAHs (*14*). Many other Gulf of Mexico pelagics may have spawned in oiled habitats, including yellowfin tuna, dolphin fish, blue marlin, and swordfish (*15*).

To more precisely define the mechanisms of crude oil cardiotoxicity and to evaluate the potential vulnerability of eggs, larvae, and juveniles in the vicinity of the DWH spill, we assessed the impact of field-collected DWH oil samples on in vitro cardiomyocyte preparations dissociated from the hearts of bluefin tuna (*T. orientalis)* and yellowfin tuna (*T. albacares*). Juvenile tunas were caught at sea and held in captivity at the Tuna Research Conservation Center and the Monterey Bay Aquarium (*16*).

The cardiotoxic effects of four distinct environmental samples of MC252 crude oil were assessed as water-accommodated fractions (WAFs) prepared in Ringer solution for marine fish (*16*). Oil samples were collected under chain of custody during the DWH spill response effort. The samples included riser "source" oil (sample 072610-03), riser oil that was "artificially weathered" by heating at 90° to 105°C (sample 072610-W-A), and two skimmed oil samples: "slick A" (sample CTC02404-02), collected 29 July 2010, and "slick B" (sample GU2888-A0719-OE701), collected 19 July 2010 by the U.S. Coast Guard cutter *Juniper*. High-energy WAFs were prepared in a commercial blender that dispersed oil droplets to mimic release conditions at the MC252 well head (*16*). As expected from previous studies (*11*, *12*), the total sum ($\sum$) of PAHs declined in WAFs from source oil to the surface-weathered samples, owing to loss of naphthalenes, whereas the total concentrations of three-ringed PAHs (e.g., phenanthrenes) increased proportionately (fig. S1 and table S1). PAH concentrations were in a range expected to cause cardiotoxicity in intact embryos and consistent with the $\sum$PAHs measured in some surface water samples during the DWH oil spill (up to 84 μg/liter) (*16*, *17*). WAFs in Ringer solution were perfused over freshly dissociated, isolated tuna cardiomyocytes, and we assessed the effects of these oil-containing solutions on excitation-contraction (EC) coupling using electrophysiological and Ca^{2+}-imaging techniques.

[1]Department of Biology, Stanford University, Hopkins Marine Station, Pacific Grove, CA 93950, USA. [2]Northwest Fisheries Science Center, National Oceanic and Atmospheric Administration, Seattle, WA 98112, USA.

*Corresponding author. E-mail: bblock@stanford.edu

Patch-clamp recordings revealed a strong effect of DWH source oil and weathered oil on bluefin and yellowfin tuna cardiomyocytes' action potential duration (APD) (Fig. 1 and fig. S3). A concentration-dependent lengthening of the APD waveform was observed in both tuna species. APD at 90% repolarization (i.e., equivalent to the QT interval on an electrocardiogram) was significantly increased across all four oil samples at $\sum$PAH concentrations ranging from 4 to 61 µg/liter (table S1). The source and weathered oils significantly decreased the APD at 10% repolarization (APD_{10}) (Fig. 1). WAF exposures did not influence other action potential parameters, such as resting membrane potential and action potential amplitude (figs. S2 and S3). This suggests that I_{K1}, the background current responsible for resting membrane potential, and I_{Na}, the current responsible for the upstroke of the action potential, are not modified by crude oil. All four oil samples significantly increased the time for repolarization from APD_{30} to APD_{90}. This increase in triangulation (Fig. 1, I to L, and fig. S3, E and F) is a strong predictor of fatal cardiac arrhythmia (18). Pharmacological agents that cause a cardiac repolarization disorder by lengthening cardiomyocyte APD, as well as congenital mutations of hERG (human *ether-à-go-go–related gene* or *KCNH2*) channels—the mammalian homolog to the fish delayed rectifier potassium current (I_{Kr}) (19)—are known to cause or aggravate ventricular arrhythmias, which can result in torsade de pointes and/or sudden death (20).

Overall, the effects of MC252 oil WAFs on cardiomyocyte action potentials in bluefin and yellowfin tunas were similar. However, the cardiotoxic potency of each oil sample correlated closely with the concentrations of three-ringed PAHs rather than total $\sum$PAHs (fig. S4), as evidenced in particular by the extensively weathered slick B sample (fig. S1 and table S1), which increased both APD and triangulation without affecting resting membrane potential or amplitude (Fig. 1 and figs. S2 and S3). In some cardiomyocytes, WAFs caused unstable action potentials after depolarizations (fig. S5B). Such arrhythmias were not observed among ventricular cells in Ringer solution over an equivalent recording duration (fig. S5A).

The functional effects of PAHs on fish cardiac rhythmicity suggest that components of crude oil interfere with EC coupling, which links electrical excitation to contraction in cardiomyocytes (21, 22). Depolarization of the cardiac sarcolemmal membrane opens voltage-gated ion channels, including L-type Ca^{2+} channels, which results in Ca^{2+} entry into the cytosol. This Ca^{2+} transient triggers the release of additional Ca^{2+} from internal stores [sarcoplasmic reticulum (SR)] by means of a Ca^{2+}-induced Ca^{2+} release mechanism (CICR) (23–25). The rise in intracellular Ca^{2+} activates the contractile machinery within the cardiomyocyte. Critical for action potential repolarization are the opening and closing of voltage-gated Na^+, Ca^{2+}, and K^+ channels, which renew the EC coupling process at every heartbeat. The repolarization of the tuna cardiomyocyte action potential involves a delicate balance of inward and outward ionic currents. Thus, cardiac action potential prolongation could be due to a decrease in outward current, an increase in inward current, or both. To distinguish between these possibilities, we used electrophysiological analyses (voltage clamp) to investigate the influence of slick B (as a representative oil sample of all four WAFs) on the major outward currents (I_K) and inward calcium current (I_{Ca}) in isolated cardiomyocytes.

We characterized the rapid component of the delayed potassium current (I_{Kr}) in the bluefin tuna using electrophysiological and pharmacological techniques as previously described (i.e., E-4031–sensitive current (26)]. In the bluefin tuna ventricular cardiomyocyte, I_{Kr} amplitude and tail current were reduced in a concentration-dependent manner in response to exposures to slick B WAF (Fig. 2, A to C) with a half maximum inhibitory concentration (IC_{50}) of 51 ± 6 µg $\sum$PAHs per liter and a Hill coefficient of 1.19 ± 0.11. Perfusion with surface oil (slick A) also decreased I_{Kr} in bluefin tuna ventricular cardiomyocytes (fig. S6) with a similar IC_{50} (53 ± 31 µg/liter) and Hill coefficient (1.16 ± 0.43). In yellowfin tuna, exposure of ventricular cardiomyocytes to slick B WAF also significantly decreased I_{Kr} tail currents $IC_{50} = 61 \pm 12$ µg/liter, Hill coefficient = 0.84 ±
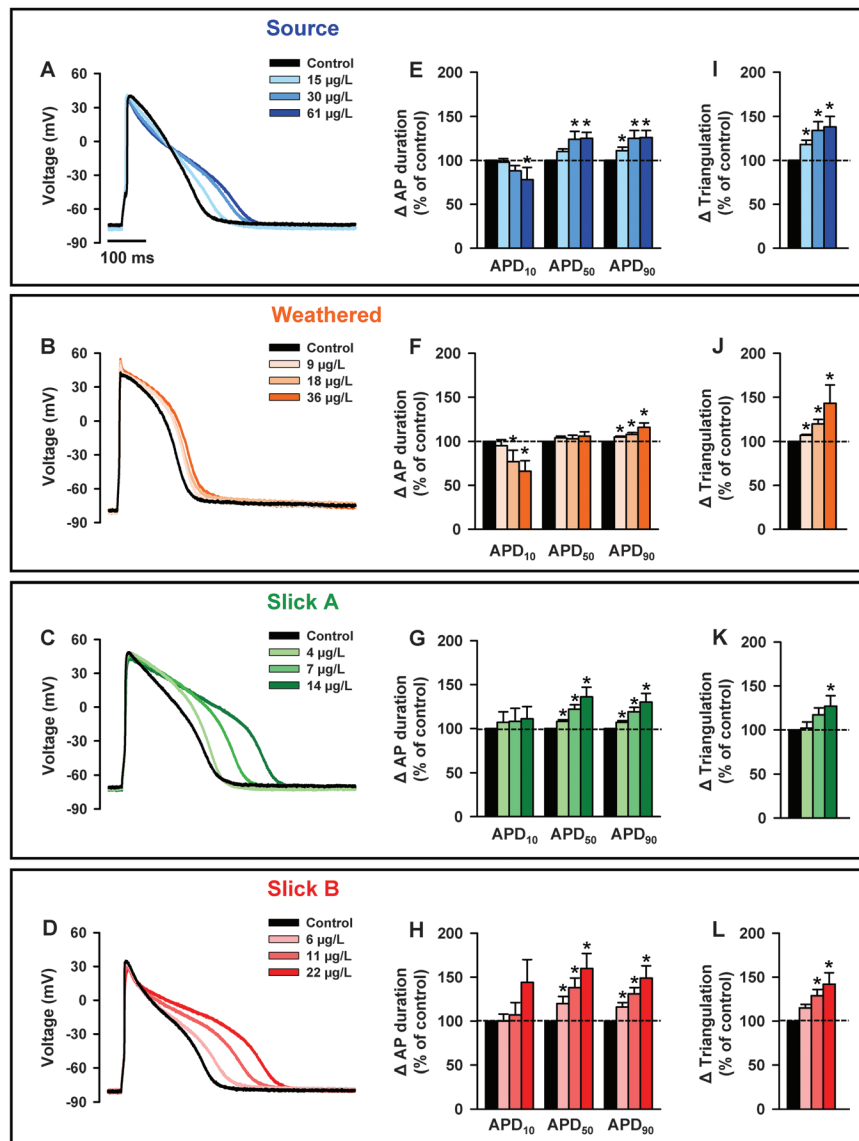

Fig. 1. Effect of oil WAFs on action potential characteristics from bluefin tuna ventricular cardiomyocytes. (A to D) Action potentials in controls (black) and with ascending concentrations of source oil (blue traces), artificially weathered (orange traces), slick A (green traces), and slick B (red traces) WAFs. **(E to H)** APD (expressed as a percentage of control) at 10, 50, and 90% repolarization in control (black bars) and with ascending concentrations of source ($n = 9$), artificially weathered ($n = 8$), slick A ($n = 7$), and slick B ($n = 7$). **(I to L)** Action potential triangulation (expressed as a percentage of control; calculated as $APD_{90} - APD_{30}$) in control (black bars) and with ascending concentrations of source, artificially weathered, slick A, and slick B. (E) to (L): Means ± SEM. *$P < 0.05$.

0.11) (fig. S7). Taken together, these data show that DWH crude oils significantly decrease I_{Kr} currents in both species. The effect of slick B (22 μg ∑PAHs per liter) on the I_{Kr} current-voltage (I-V) relation is shown in Fig. 2D. WAF perfusion reduced I_{Kr} amplitudes across all voltages without affecting the shape of the I-V curve (Fig. 2E). In addition, I_{Kr} tail currents were decreased at all voltages without shifting the curve (Fig. 2F). Bluefin tuna ventricular cardiomyocytes exposed to source oil (61 μg/liter) and yellowfin tuna ventricular cardiomyocytes exposed to slick B (22 μg/liter) showed comparable blockade of I_{Kr} (figs. S8 and S9). Thus, dissolved constituents of MC252 crude oil do not affect the voltage-dependent (gating) properties of the K+ channel but rather inhibit outward conductance in the open state, most likely by blocking the K+ channel pore. This mechanism would be consistent with the observed prolongation of the cardiomyocyte action potential. To confirm this, we perfused tuna ventricular cardiomyocytes with the specific I_{Kr} blocker, E-4031 (2 μM in Ringer solution). As anticipated, E4031 significantly prolonged APD_{90}, consistent with I_{Kr} shaping the repolarization of bluefin and yellowfin tuna cardiomyocytes (fig. S10).

I_{Ca} also plays a critical role in cardiomyocyte APD (27, 28). Exposure to the weathered slick B surface sample significantly decreased the amplitude of I_{Ca} (Fig. 3, A to C) in a concentration-dependent manner, with an IC_{50} of 36 ± 7 μg ∑PAHs per liter and a Hill coefficient of 0.76 ± 0.13 for bluefin tuna cardiomyocytes. Note that slick B WAF also slowed the inactivation decay of I_{Ca} (Fig. 3, D and E) and thereby allowed more Ca^{2+} entry during depolarization (27). As indicated by quantification of Ca^{2+} entry, there was a small, but not significant, decrease in charge passing through the channel during the square pulse (Fig. 3, F and G). I-V relations (Fig. 3H) revealed an inhibitory effect of slick B WAF on I_{Ca} across all voltages, with a slight influence on the shape of the I-V curve (Fig. 3I, top), which suggested a change in the voltage-dependent properties of Ca^{2+} channels. Perfusion with the slick B WAF shifted the activation curve toward more hyperpolarized potentials (by ~7 mV) (Fig. 3I, bottom), which allowed more Ca^{2+} entry at negative potentials. As with bluefin tuna, slick B WAF (22 μg ∑PAHs per liter) also inhibited I_{Ca} in ventricular cardiomyocytes of yellowfin tuna (IC_{50} = 46 ± 5 μg/liter, Hill coefficient = 1.01 ± 0.09) (fig. S11).

To further explore the influence of DWH oil on the voltage-dependent properties of cardiac Ca^{2+} channels, I_{Ca} was measured in bluefin cardiomyocytes with Ba^{2+} as a charge carrier. In the absence of Ca^{2+}-dependent inactivation, the channel inactivates primarily via voltage-dependent processes (27). Similar to the effects on I_{Ca}, slick B WAF significantly decreased the amplitude of I_{Ba} but did not slow the inactivation of the current (fig. S12). This suggests that the observed change in I_{Ca} inactivation rate in re-

sponse to oil is Ca^{2+}-dependent and not voltage-dependent. The decrease in I_{Ca} amplitude and slowing of inactivation might have countervailing effects on Ca^{2+} entry during the plateau phase of the action potential, as measured from action potential waveforms in response to physiological pulses (29).

The entry of Ca^{2+} via I_{Ca} during action potentials was similar among controls and ventricular cardiomyocytes perfused with slick B WAF (22 μg ∑PAHs per liter) for bluefin (fig. S13) and yellowfin tunas (fig. S14). Overall, the absence of an effect of crude oil on Ca^{2+} entry during a physiological pulse is attributable to (i) an increase in APD, allowing more time for Ca^{2+} entry; (ii) a leftward shift in the activation properties of Ca^{2+} channels; and (iii) a slowing of I_{Ca} inactivation. Although our findings are not sufficient to explain action potential prolongation, they show that DWH crude oil significantly decreases I_{Ca} amplitude in cardiomyocytes of tunas. L-type Ca^{2+} channels play a key role in initiating the critical CICR from SR internal stores; thus, the next series of experiments were designed to measure whole-cell Ca^{2+} cycling in isolated cardiomyocytes exposed to DWH oils.

Intracellular Ca^{2+} transients in bluefin tuna cardiomyocytes were recorded using confocal microscopy and Ca^{2+}-sensitive dye (Fluo-4). Exposures to each oil sample (source, artificially weathered source, slick A, and slick B at 30, 18, 7, and 11 μg ∑PAHs per liter, respectively) significantly decreased the Ca^{2+} transient amplitudes and slowed the decay of the Ca^{2+} transients in bluefin tuna ventricular cardiomyocytes (Fig. 4). This reduction in Ca^{2+} transient amplitudes would decrease contractility and would reduce cardiac output at the scale of the whole heart. A diminished cytosolic Ca^{2+} transient could be a consequence of reduced extracellular Ca^{2+} influx, a smaller Ca^{2+} release from SR internal stores, or both (24, 30).

The direct measurements of Ca^{2+} transients in cardiomyocytes indicate there may be inhibitory effects of oil on SR Ca^{2+} release and/or reuptake. To investigate the possible SR sites of interaction, cardiomyocytes were exposed to pharmacological inhibitors of SR Ca^{2+} release channels (5 μM ryanodine) and Ca^{2+} adenosine triphosphatase (ATPase) pumps (2 μM thapsigargin) for at least 30 min before exposures to WAFs. Under pharmacological blockade, the four dis-
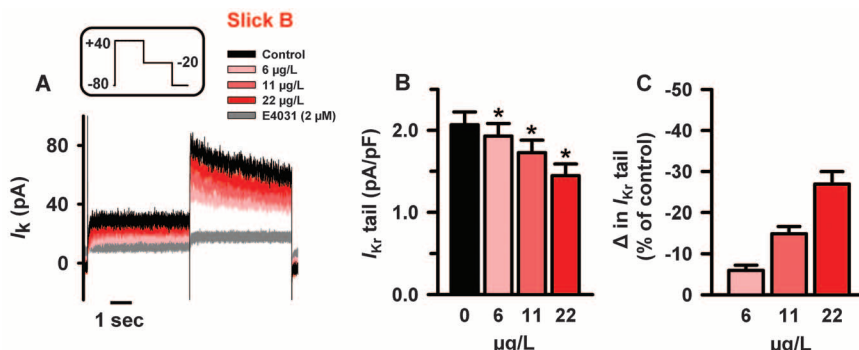

Fig. 2. Effect of oil WAF (slick B) on K+ current (I_K) from bluefin tuna ventricular cardiomyocytes. (A) I_K recorded in control condition (black trace), with ascending concentrations of slick B WAF (red traces) or the I_K blocker E4031 (2 μM, gray trace). (Inset) Voltage step to record I_K. **(B)** I_{Kr} tail in control (black bar) and with ascending concentrations of slick B (red bars, n = 9). **(C)** Change in I_{Kr} tail (expressed as a percentage of control) with ascending concentrations of slick B. **(D)** I-V relation of I_K in control (black trace), slick B (22 μg/liter, red trace), and with E4031 (2 μM, gray trace). **(E** and **F)** I-V relation of I_{Kr} [circle in (E)] and tail I_{Kr} [triangle in (F)] in control (black trace) and with slick B (22 μg/liter, red trace, n = 9). (B), (C), (E), and (F): Means ± SEM. *P < 0.05.
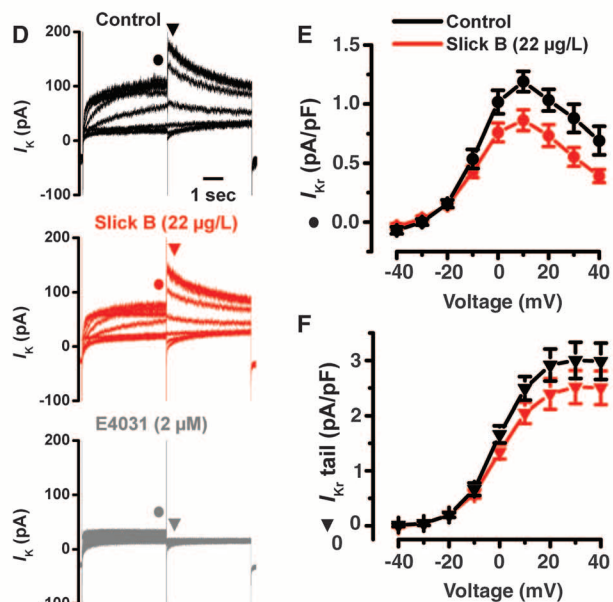
tinct crude oil samples had no significant effect on the amplitude of the cytosolic Ca^{2+} transient (Fig. 4D). This indicates that the oil-induced decrease in Ca^{2+} transient amplitude observed in the absence of blockers is due to a disruption of SR Ca^{2+} release and/or reuptake from internal stores. However, these toxic effects of oil on intracellular Ca^{2+} cycling were partially offset by

an additional influx of I_{Ca} via L-type Ca^{2+} channels during action potential prolongation, consistent with the I_{Ca} results in Fig. 3.

Our experimental findings provide a mechanistic underpinning for cardiac-specific physiological defects previously reported and reinforce the findings that crude oil has deleterious physiological impacts on fish hearts (10). Our results

with crude oil are similar to the physiological effects of the antimalarial drug halofantrine, a chemical with structural similarities to three-ringed PAHs that causes K^+ channel inhibition and cardiac arrhythmias (31). Our results indicate compounds in DWH oil produce a cardiotoxic mechanism that have direct effects on ion channels involved in the EC coupling and cardiac
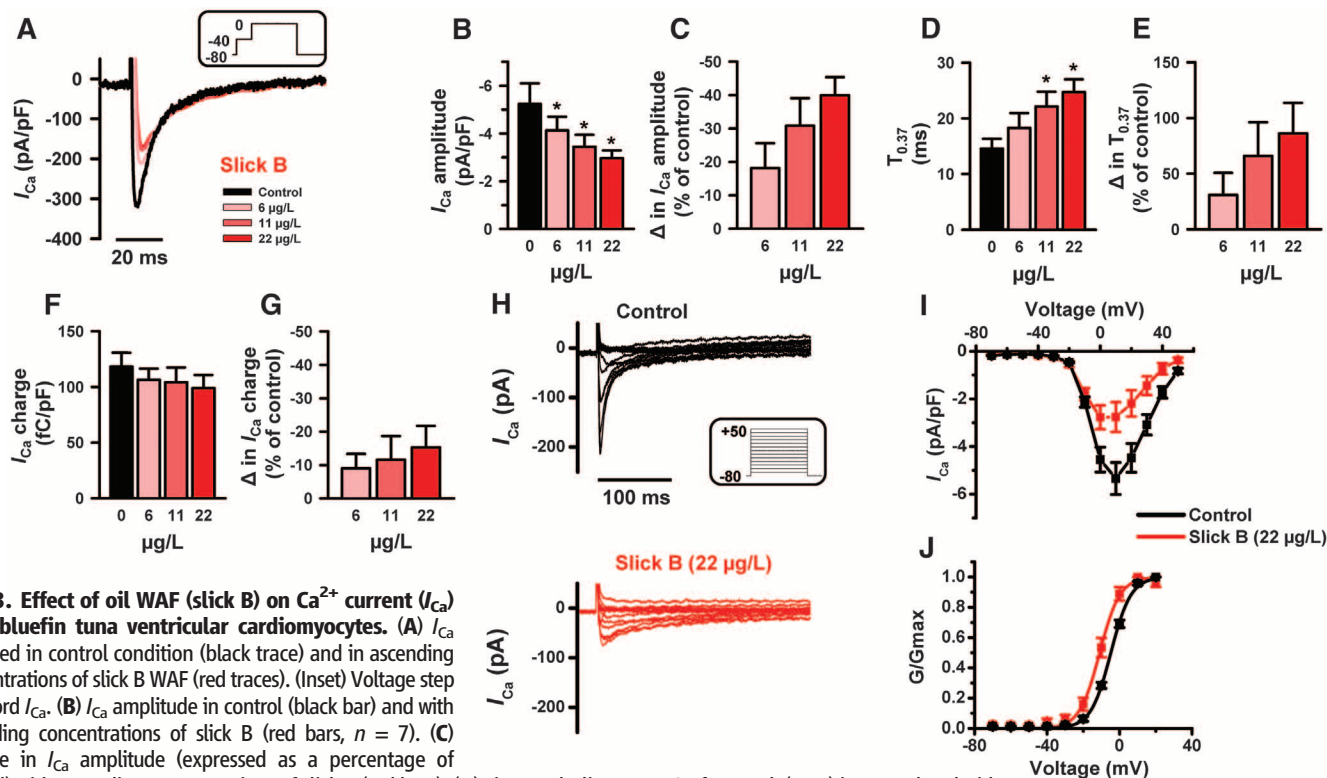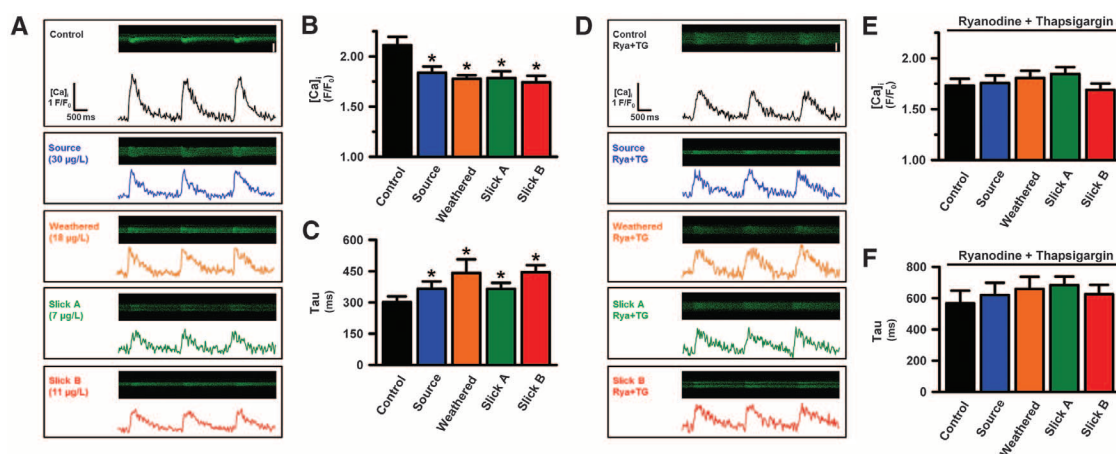

Fig. 3. Effect of oil WAF (slick B) on Ca^{2+} current (I_{Ca}) from bluefin tuna ventricular cardiomyocytes. (**A**) I_{Ca} recorded in control condition (black trace) and in ascending concentrations of slick B WAF (red traces). (Inset) Voltage step to record I_{Ca}. (**B**) I_{Ca} amplitude in control (black bar) and with ascending concentrations of slick B (red bars, $n = 7$). (**C**) Change in I_{Ca} amplitude (expressed as a percentage of control) with ascending concentrations of slick B (red bars). (**D**) Time to decline to 37% of I_{Ca} peak ($T_{0.37}$) in control and with ascending concentrations of slick B. (**E**) Change in $T_{0.37}$ (expressed as a percentage of control) with ascending concentrations of slick B (red bars). (**F**) I_{Ca} charge in control and with ascending concentrations of slick B. (**G**) Change in I_{Ca} charge (expressed as a percentage of control) with ascending concentrations of slick B WAF. (**H**) I-V relations of I_{Ca} in control condition (black trace) and with slick B (22 µg/liter, red trace). (Inset) Voltage step to record I_{Ca}. (**I**) I-V relation of I_{Ca} in control (black trace) and with slick B (22 µg/liter, red trace, $n = 7$). (**J**) Availability-voltage relation (normalized conductance G/G_{max}) of I_{Ca} in control and with slick B (22 µg/liter, $n = 7$). (B) to (G), (I), and (J): Means $\pm$ SEM. *$P < 0.05$.

Fig. 4. Effect of oil WAFs on Ca^{2+} transients from bluefin tuna ventricular cardiomyocytes. (**A**) Ca^{2+} transients recorded in control (black trace) and with source (30 µg/liter, blue trace); artificially weathered (18 µg/liter, orange trace); slick A (7 µg/liter, green trace); and slick B (11 µg/liter, red trace) WAFs, respectively. (**B**) Ca^{2+} transients amplitude as fluorescence divided by baseline fluorescence (F/F_0) and (**C**) tau, the decay time constant of Ca^{2+} transients, in control ($n = 37$) and source ($n = 29$), artificially weathered ($n = 27$), slick A ($n = 25$), and slick B ($n = 21$), respectively. (**D**) Ca^{2+} transients recorded in ryanodine (Rya) and thapsigargin (Tg) (black trace) and with source (30 µg/liter, blue trace); artificially weathered (18 µg/liter, orange trace); slick A (7 µg/liter, green trace);

and slick B (11 µg/liter, red trace), respectively. (**E**) Ca^{2+} transients amplitude (F/F_0) and (**F**) tau of decay of Ca^{2+} transients in ryanodine and thapsigargin ($n = 22$) and source ($n = 17$), artificially weathered ($n = 18$), slick A ($n = 17$), and slick B ($n = 16$), respectively. (B), (C), (E), and (F): Means $\pm$ SEM. *$P < 0.05$.

contractility of cardiomyocytes. These pathways in cardiac muscle cells are highly conserved across all vertebrates, which explains the common, canonical crude oil toxicity syndrome observed in a diversity of fish species from habitats that range from tropical freshwater (zebrafish) to boreal marine (herring).

In conclusion, the oil-induced disruption of cardiomyocyte repolarization via K^+ channel blockade and sarcolemmal and SR Ca^{2+} cycling should call attention to a previously underappreciated risk to wildlife and humans, particularly from exposure to cardioactive PAHs that are also relatively enriched in air pollution. I_{Kr} inhibition by DWH crude oil from the MC252 well was robust, and its properties are consistent with direct channel pore block. These K^+ channel targets and their unique gating properties play a critical role in cardiac action potential repolarization and are highly conserved across the animal kingdom (20). These results lead us to believe that PAH cardiotoxicity was potentially a common form of injury among a broad range of species during and after the DWH oil spill. The early life stages of fish and other vertebrates may have been particularly vulnerable, given that even a transient and sublethal effect of PAHs on the embryonic heartbeat can cause permanent secondary changes in heart shape and cardiac output (32). Moreover, the underlying ion channel currents that drive the electrical properties of cardiomyocytes in tunas and mammals (such as heart rates), are similar (26, 33). Thus, we suggest the extension of our current oil toxicity results to mammalian, cardiomyocytes may be warranted to better understand PAH threats to human health.

References and Notes

1. M. G. Carls, J. P. Meador, *Hum. Ecol. Risk Assess. Int. J.* **15**, 1084–1098 (2009).
2. C. H. Peterson et al., *Science* **302**, 2082–2086 (2003).
3. C. E. Boström et al., *Environ. Health Perspect.* **110** (suppl. 3), 451–488 (2002).
4. J. J. Stegeman, J. J. Lech, *Environ. Health Perspect.* **90**, 101–109 (1991).
5. J. P. Incardona et al., *Proc. Natl. Acad. Sci. U.S.A.* **109**, E51–E58 (2012).
6. M. G. Carls, S. D. Rice, J. E. Hose, *Environ. Toxicol. Chem.* **18**, 481 (1999).
7. R. A. Heintz, J. W. Short, S. D. Rice, *Environ. Toxicol. Chem.* **18**, 494 (1999).
8. J. P. Incardona, T. K. Collier, N. L. Scholz, *Toxicol. Appl. Pharmacol.* **196**, 191–205 (2004).
9. J. P. Incardona et al., *Environ. Health Perspect.* **113**, 1755–1762 (2005).
10. J. P. Incardona et al., *Environ. Sci. Technol.* **43**, 201–207 (2009).
11. J. H. Jung et al., *Chemosphere* **91**, 1146–1155 (2013).
12. J. P. Incardona, T. K. Collier, N. L. Scholz, *J. Expo. Sci. Environ. Epidemiol.* **21**, 3–4 (2011).
13. J. D. Neilson, S. E. Campana, *Can. J. Fish. Aquat. Sci.* **65**, 1523–1527 (2008).
14. B. A. Block et al., *Nature* **434**, 1121–1127 (2005).
15. J. R. Rooker et al., *PLOS ONE* **7**, e34180 (2012).
16. Materials and methods are available as supplementary materials on *Science* Online.
17. A. R. Diercks et al., *Geophys. Res. Lett.* **37**, L20602 (2010).
18. L. M. Hondeghem, L. Carlsson, G. Duker, *Circulation* **103**, 2004–2013 (2001).
19. J. M. Nerbonne, R. S. Kass, *Physiol. Rev.* **85**, 1205–1253 (2005).
20. P. Kannankeril, D. M. Roden, D. Darbar, *Pharmacol. Rev.* **62**, 760–781 (2010).
21. D. M. Bers, *Nature* **415**, 198–205 (2002).
22. M. B. Cannell, H. Cheng, W. J. Lederer, *Science* **268**, 1045–1049 (1995).
23. H. A. Shiels, E. V. Freund, A. P. Farrell, B. A. Block, *J. Exp. Biol.* **202**, 881–890 (1999).
24. H. A. Shiels, A. Di Maio, S. Thompson, B. A. Block, *Proc. Biol. Sci.* **278**, 18–27 (2011).
25. M. Vornanen, H. A. Shiels, A. P. Farrell, *Comp. Biochem. Physiol. A Mol. Integr. Physiol.* **132**, 827–846 (2002).
26. G. L. Galli, M. S. Lipnick, B. A. Block, *Am. J. Physiol. Regul. Integr. Comp. Physiol.* **297**, R502–R509 (2009).
27. F. Brette, J. Leroy, J. Y. Le Guennec, L. Sallé, *Prog. Biophys. Mol. Biol.* **91**, 1–82 (2006).
28. F. Brette et al., *Biochem. Biophys. Res. Commun.* **374**, 143–146 (2008).
29. F. Brette, L. Sallé, C. H. Orchard, *Biophys. J.* **90**, 381–389 (2006).
30. H. A. Shiels, E. White, *Am. J. Physiol. Regul. Integr. Comp. Physiol.* **288**, R1756–R1766 (2005).
31. H. Tie et al., *Br. J. Pharmacol.* **130**, 1967–1975 (2000).
32. C. E. Hicken et al., *Proc. Natl. Acad. Sci. U.S.A.* **108**, 7086–7090 (2011).
33. J. M. Blank et al., *J. Exp. Biol.* **207**, 881–890 (2004).

Massively Parallel Single-Cell RNA-Seq for Marker-Free Decomposition of Tissues into Cell Types

Diego Adhemar Jaitin,[1]* Ephraim Kenigsberg,[2,3]* Hadas Keren-Shaul,[1]* Naama Elefant,[1] Franziska Paul,[1] Irina Zaretsky,[1] Alexander Mildner,[1] Nadav Cohen,[2,3] Steffen Jung,[1] Amos Tanay,[2,3]†‡ Ido Amit[1]†‡

In multicellular organisms, biological function emerges when heterogeneous cell types form complex organs. Nevertheless, dissection of tissues into mixtures of cellular subpopulations is currently challenging. We introduce an automated massively parallel single-cell RNA sequencing (RNA-seq) approach for analyzing in vivo transcriptional states in thousands of single cells. Combined with unsupervised classification algorithms, this facilitates ab initio cell-type characterization of splenic tissues. Modeling single-cell transcriptional states in dendritic cells and additional hematopoietic cell types uncovers rich cell-type heterogeneity and gene-modules activity in steady state and after pathogen activation. Cellular diversity is thereby approached through inference of variable and dynamic pathway activity rather than a fixed preprogrammed cell-type hierarchy. These data demonstrate single-cell RNA-seq as an effective tool for comprehensive cellular decomposition of complex tissues.

Understanding the heterogeneous and stochastic nature of multicellular tissues is currently approached through a priori defined cell types that are used to dissect cell populations along developmental and functional hierarchies (1–3). This methodology heavily relies on enumeration of cell types and their precise definition, which can be controversial (4–7) and is based in many cases on indirect association of function with cell-surface markers (5–8). Perhaps the best understood model for cellular differentiation and diversification is the hematopoietic system. The developmental tree branching from hematopoietic stem cells toward distinct immunological functions was carefully worked out through many years of study, and effective cell-surface markers are available to quantify and sort the major hematopoietic cell types. Even in this well-explored system, however, it is becoming increasingly difficult to explain modern genome-wide and in vivo data with refined cell types' hierarchy and functions that extend beyond the classical myeloid and lymphoid cell types. For example, dendritic cells (DCs) are antigen-presenting

[1]Department of Immunology, Weizmann Institute, Rehovot 76100, Israel. [2]Department of Computer Science and Applied Mathematics, Weizmann Institute, Rehovot 76100, Israel. [3]Department of Biological Regulation, Weizmann Institute, Rehovot 76100, Israel.

*These authors contributed equally to this work.
†These authors contributed equally to this work.
‡Corresponding author. E-mail: amos.tanay@weizmann.ac.il (AT); ido.amit@weizmann.ac.il (IA)